SANDIA REPORT

SAND2001-3361
Unlimited Release
Printed November 2001

Wire Initiation Studies at the University of Nevada-Reno: An LDRD Report

Melissa R. Douglas and Bruno Bauer

Prepared by
Sandia National Laboratories
Albuquerque, New Mexico 87185 and Livermore, California 94550

Sandia is a multiprogram laboratory operated by Sandia Corporation, a Lockheed Martin Company, for the United States Department of Energy under Contract DE-AC04-94AL85000.

Issued by Sandia National Laboratories, operated for the United States Department of Energy by Sandia Corporation.

Available to DOE and DOE contractors from
U.S. Department of Energy
Office of Scientific and Technical Information
P.O. Box 62
Oak Ridge, TN 37831

Telephone: (865)576-8401
Facsimile: (865)576-5728
E-Mail: reports@adonis.osti.gov
Online ordering: http://www.doe.gov/bridge

Available to the public from
U.S. Department of Commerce
National Technical Information Service
5285 Port Royal Rd
Springfield, VA 22161

Telephone: (800)553-6847
Facsimile: (703)605-6900
E-Mail: orders@ntis.fedworld.gov
Online order: http://www.ntis.gov/ordering.htm

SAND2001-3361
Unlimited Release
Printed November 2001

Wire Initiation Studies at the University of Nevada-Reno: An LDRD Report

Melissa R. Douglas
Z-Pinch Physics and Power Flow Department
Sandia National Laboratories
P.O. Box 5800
Albuquerque, New Mexico 87185-1194

Bruno Bauer, Assistant Professor
Department of Physics
University of Nevada
Reno, Nevada

ABSTRACT

Wire explosion experiments have been carried at the University of Nevada, Reno. These experiments investigated the explosion phase of wires with properties and current-driving conditions comparable to that used in the initial stage of wire array z-pinch implosions on the Z machine at Sandia National Laboratories. Specifically, current pulses similar to and faster than the pre-pulse current on Z (current prior to fast rise in current pulse) were applied to single wire loads to study wire heating and the early development of plasmas in the wire initiation process. Understanding such issues are important to larger pulsed power machines that implode cylindrical wire array loads comprised of many wires. It is thought that the topology of an array prior to its acceleration influences the implosion and final stagnation properties, and therefore may depend on the initiation phase of the wires. Single wires ranging from 4 to 40 μm in diameter and comprised of material ranging from Al to W were investigated. Several diagnostics were employed to determine wire current, voltage, total emitted-light energy and power, along with the wire expansion velocity throughout the explosion. In a number of cases, the explosion process was also observed with x-ray backlighting using x-pinches. The experimental data indicates that the characteristics of a wire explosion depend dramatically on the rate of rise of the current, on the diameter of the wire, and on the heat of vaporization of the wire material. In this report, these characteristics will be described in detail. Of particular interest is the result that a faster current rise produces a higher energy deposition into the wire prior to explosion. This result introduces a different means of increasing the efficiency of wire heating. In this case, the energy deposition along the wire and its subsequent expansion, is uniform compared to a "slow" current rise (170 A/ns compared to 22 A/s current rise into a short circuit) and the expansion velocity is larger. The energy deposition and wire expansion is further modified by the wire diameter and material. Investigations of wire diameter indicate that the diameter primarily effects the expansion velocity and energy deposition; thicker wires explode with greater velocities but absorb less energy per atom. The heat of vaporization also categorizes the wire explosion; wires with a low heat of vaporization expand faster and emit less radiation than their high heat of vaporization counterparts.

I. Introduction

The University of Nevada, Reno, is home to Zebra (HDZP-II), a pulsed power device that can produce and confine hot, dense plasmas simply and efficiently. The source of these plasmas is the z-pinch, a method of plasma production in which a large current is applied axially to a load, often in the form of a single wire or cylindrical wire array. The load is compressed, heated, and confined by strong current-produced magnetic fields, creating for a short time plasma environments similar to those of stellar interiors. Z-pinches are copious x-ray radiation sources and, as such, can be used for a variety of applications ranging from inertial confinement fusion to material response of x-ray emissions. They also offer a means to study the fundamental nature of plasmas.

Recent experiments on the 11MJ Z machine at Sandia National Laboratories have produced world-record x-ray radiation energy and powers. In particular, powers of over 250 TW and total x-ray energies of over 1.8 MJ have been achieved on few ns timescales using small diameter (less than 40 mm) nested tungsten wire arrays driven by a 18 MA peak current. This has generated a renaissance in the field of z-pinches, particularly in applications concerning fusion. Even with such successes, the details of the z-pinch evolution, from the formation of an initial plasma state, to the dynamics of the implosion, to the plasma properties at final stagnation, is not well diagnosed or understood. For this reason, it can be difficult to efficiently optimize a z-pinch system for the desired radiation output since the detailed physics is not well known; much effort can be spent on trouble-shooting. This can be financially costly and time consuming on larger, pulsed power drivers where only one experimental shot per day can be accomplished. To this end, smaller, less expensive pulsed power generators, such as Zebra, are extremely useful in examining a particular aspect of z-pinch physics, i.e., the initiation process of a single wire or a broad scan of a fundamental pinch parameter.

Although Z pinch loads come in many forms, including gas puffs, wire arrays, and thin cylindrical foils, the most common z-pinch load is the wire array. On the Z machine, wire arrays range in diameter from 10 to 60 mm, and are comprised of anywhere from 50 to 300 wires. The wire diameter is small, typically between 4 to 30 μm and the wire material ranges from Al to W in composition. For high wire numbers (>180), the array is believed to form a shell-like distribution resulting from the coronal merging of adjacent exploding wires. For smaller wire numbers, the array is believed to maintain a complex three-dimensional topology throughout the implosion. In this latter case, a substantial precursor material can form between the array and stagnation axis, caused by evaporation of wire material and magnetic pressure. This effect, along with azimuthal perturbations formed by the discrete nature of the array, can alter the dynamics of the implosion; the pinch characteristics at stagnation may be very different compared to a high wire number case.

Whether the array develops a shell-like nature, retains its individual wire topology with a downstream mass distribution, or behaves in a manner somewhere in between these two scenarios is of great interest, since this defines the implosion phase and stagnation characteristics of the pinch. It is most likely that the initial topology of the array depends on the initiation phase of the wires. The process by which the wires explode, the perturbations that develop at this time in both the wire core and corona (thermal or sausage instabilities), and the expansion velocity of both the core and corona,

dictate the manner in which the pinch implodes and define issues which limit pinch performance. For example, any z-pinch that is shell-like in nature, such as annular gas puffs or cylindrical foils, is susceptible to the Magneto-Rayleigh Taylor (MRT) instability during the implosion phase. This instability develops at the plasma-vacuum interface and can keep the plasma from reaching high densities and temperatures at stagnation. The MRT instability has been directly observed in pinhole images of gas puffs and optical framing camera images of thin foil loads. It is believed to occur in high wire number arrays although the early stages of wire array initiation has not yet been diagnosed in such cases (the instability is observed in late-time x-ray pin-hole images). For wire arrays, the initial seed for the instability has yet to be determined, and the growth rate of the instability has not been measured. The initial seed has been speculated to form from the superposition of individual wire instabilities once a global magnetic field has been established. One of the roles of Zebra will be to thoroughly investigate the early evolution of exploding single wires and that of small wire number arrays in hopes of illuminating the dominant physical processes that occur during initiation and influence the rest of the pinch implosion.

Presented here is an investigation of the initial stages of wire explosions. Current pulses similar to the prepulse at Sandia's Z-facility has been applied to single-wire loads to acquire information about the expansion of exploding wires and the early development of plasmas in wire-array z-pinches. It should be noted that the physics of the wire explosion process during the Z prepulse may be overshadowed by the effects of the main current pulse, which continues to drive the array physics during the first 50 ns or so prior to array acceleration. Nonetheless, this work is of interest in that many of the physical processes most likely scale on some level to higher current machines. Several diagnostics have been employed to determine wire current, voltage, total emitted-light energy and power, and wire-expansion velocity throughout the explosion. These diagnostics are presented and discussed, along with some initial treatment of the experimental results and plans for future experiments.

2. Explosion of wires driven by Z-like and faster prepulses

The heating and expansion of single wires with current prepulses similar to, and faster than that of the Z generator at Sandia National Laboratories (SNL) has been investigated. Individual W, Mo, Ti, Ni, Fe, Au, Cu, Al, Ag, and Au-plated W wires ranging in diameter from 4 to 40 μm were exploded using a fast kiloampere pulse fed from a 9-m-long 50-ohm coax. The wire current, voltage, emitted light, and wire expansion velocity were measured as a function of time with electrical, optical, and laser diagnostics throughout the explosion. A number of the exploding wires were also observed with x-ray backlighting resulting from several x-pinch backlighters, and with gated optical imaging.

2.1 Experimental Setup

The details of the experiment, including a schematic of the diagnostic setup, is shown in Figure 1. A 50-kV Maxwell 40167 trigger amplifier triggers a 100-kV

Maxwell 40151-B pulse generator with a stored energy of 12.6 J that provides the current and voltage used to drive the wire explosions. A 50-Ω, 9-m coaxial transmission line delivers the positive-voltage pulse from the generator to the wire. The setup produces a fast pulse with a 170 A/ns current rise into a short-circuit, or, with an inductor inserted before the generator output, a slower pulse with a 22 A/ns current rise into a short-circuit. The slower rise is characteristic of the prepulse through individual wires on Z (7kA/ns applied for 50 ns to an array of 240-300 fine wires). For the results presented here, the electrical pulse was applied to a single wire 2 cm in length with a diameter ranging from 4 to 40 μm. The wire formed the central conductor of a coaxial line which was evacuated to a pressure of ~10^{-5} torr before the explosion (to prevent arcing between the anode and the cathode or surrounding coaxial ground).

The current flowing through the wire itself was measured with a 2-GHz bandwidth shunt resistor, while the voltage drop across the wire was measured with a low inductance, passive high-voltage probe (100kV, 1.5ns rise time). The current into the wire and the voltage at the output of the transmission line were also measured using Bdot and Ddot probes, respectively. From the current and voltage data, the resistive component of the voltage, the load resistance, and the joule heating of the load could be determined throughout the wire explosion. The difference between the current entering the anode-side of the wire and leaving the cathode-side of the wire was also measured; this corresponds to current lost through arcing to the return-current outer conductor.

The evolution of optical energy emitted from the exploding wire was monitored by a PIN diode with a rise time of less than 1 ns. The diode is one focal length behind a large collecting lens, so that the efficiency of light collection is equal for all points in the plasma, within a 1-cm wide by 2-cm long window. This provided comparative information on the emitted-optical power of different wire substances and diameters.

The essential features of the wire expansion, including the start of the explosion, the expansion velocity, and the electron plasma temperature and density were investigated using streak camera images, interferometry, shadowgraphy and imaging spectroscopy. Streak camera (Hamamatsu C-1587-01) shadow images of the wire during the explosion were obtained using a high-power diode laser (905 nm, 10 W, 200 ns, 0.1 ns jitter) as a backlighter. These images were used to determine plasma expansion velocity (at the sharp plasma density jump from 10^{20} cm^{-3} to an order of magnitude higher or more) and the starting time of the explosion. For both the interferometry and shadowgraphy, a Q-switched Nd-glass laser (527 nm, 100 mJ, 20 ns) probed the plasma. The images of wire explosions were then captured on a CCD camera. Electron densities were measured using an air-wedge shearing interferometer[1], consisting of two 3-degree glass wedges placed between a lens and the CCD camera. The wedges were pressed together, forming a small air gap between them. The reflected beams from the two internal faces of the gap created an interference pattern in the overlapped region in the imaging plane. Electron temperatures were estimated using an optical imaging spectrometer (Chromex 500is with a 100 grooves/mm grating, recorded by a CCD camera).

[1] G.S. Sarkisov, Shearing interferometer with an air wedge for the electron density diagnostics in a dense plasma, Instr. Exp. Techniques, **3** , No.5, 727-731 (1996).

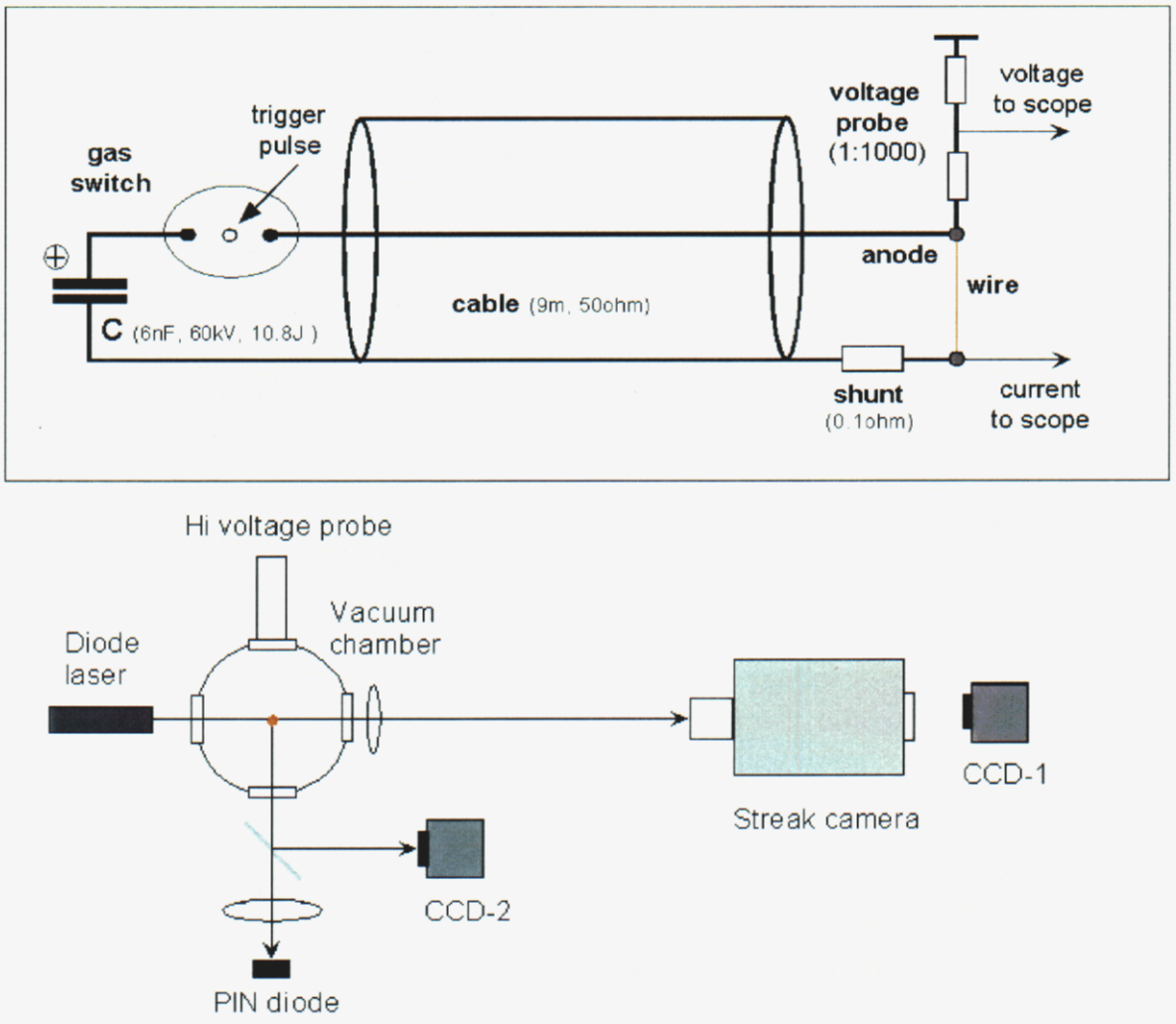

Figure 1. Experimental Setup including diagnostic configuration.

The current, voltage, PIN diode, and streak-camera-sync-output waveforms are captured by a 4-channel, 1-GHz digital scope (Tektronix TDS 684C, 5 GS/s), with a time axis cross-correlated to that of the streak camera images

2.2 Experimental results

As will be discussed in detail in the following sections, the characteristics of a wire explosion is observed to depend dramatically on the rate of rise of the current, on the diameter of the wire, and on the heat of vaporization of the wire material. Details of W wire explosions focusing on the first two issues are presented in section 2.2a, followed by brief discussions of other wire materials (section 2.2b). Since the experimental results show that there is a considerable difference in explosion properties depending on the heat of vaporization, wires studied in this latter case were grouped into two categories: wire material which has a high heat of vaporization (W, Mo, Ti, Ni, Fe) and that which has a

low heat of vaporization (Au, Cu, Al, Ag). Au-plated W wires, which were also exploded, represent an interesting combination of these two material types. The experimental results for this composite wire is included in this section.

2.2.a Tungsten wire explosions: slow and fast-rising pulse, changing diameter

Typical time-integrated images of exploding 16.2-μm diameter, 2-cm long W wires (Fig.2) show large differences in the energy deposition structure between the explosions driven by fast and slow pulses. The fast pulse produces a homogeneous "cylindrical" (Fig.2a) or "conical" (Fig.2b) structure, or explosion, in visible light. In the case of a cylindrical explosion, there is no dependence of emitted light intensity on axial location suggesting uniform deposition of energy along the wire. The "conical" explosion appears to be wider at the anode and narrower at the cathode, suggesting more energy is deposited at the anode. The slow pulse, on the other hand, results in many arcs between the positively charged wire and the ground cylinder 2.8 cm away, as illustrated in Fig. 2c. In this slow pulse case, parts of the wire never vaporize, even at late times (Fig.2d). For the cylindrical and the conical explosion modes, the region surrounding the wire glows brightly. With the slow pulse mode, the light emission is over an order of magnitude less, and comes mostly from the arcs.

The velocity of expansion is far greater for the fast pulse explosion than for the slow pulse case as shown in the streak camera images of Fig.3. (Fig. 3 data corresponds to that shown in Fig. 2). The velocity of expansion in the middle of the 16.2-μm diameter W wire is 0.83 km/s for the fast cylindrical explosion mode (Figs. 3a, 2a), 0.59 km/s for the fast conical explosion mode (Figs. 3b, 2b), and 0.15 km/s for the slow-pulse explosion (Figs. 3c, 2c). In the slow-pulse explosion, the wire expands only in the region where the off-axis arcing is absent. (The wire does not vaporize in the region with off-axis arcing.) The wire begins to expand after the voltage reaches the maximum value, i.e., after flashover. The expansion proceeds at a constant speed, indicating minimal heating of the wire after flashover.

Using a laser interferogram, the electron density was estimated at the initial stage of a fast-exploding 12.7-μm-diameter W wire. A cylindrical expansion of the wire is observed, as with the streak camera images (no disturbance of the interference fringes 65 ns and 140 ns after the start of the current pulse). The electron density was determined to have a value less than 10^{19} cm^{-3} in the outer region of the wire.

The temporal evolution of the current (1,heavy solid curve), voltage (2), and deposited joule energy (3, dashed curve) for a fast pulse cylindrical explosion and a slow pulse explosion is shown in Fig. 4. In both cases, the voltage reaches a maximum and then collapses in a few ns to a very small value, when flashover occurs. The power into the load is 7 times greater for the fast pulse than for the slow one, peaking at 60 MW in the first case, and at 9 MW in the latter. The time to flashover, from the start of the pulse, is only a little shorter (30 ns vs. 40 ns) for the fast-rising pulse than for the slow one. The result is that 3 times more energy is absorbed by the wire, when it is driven by the fast-rising pulse.

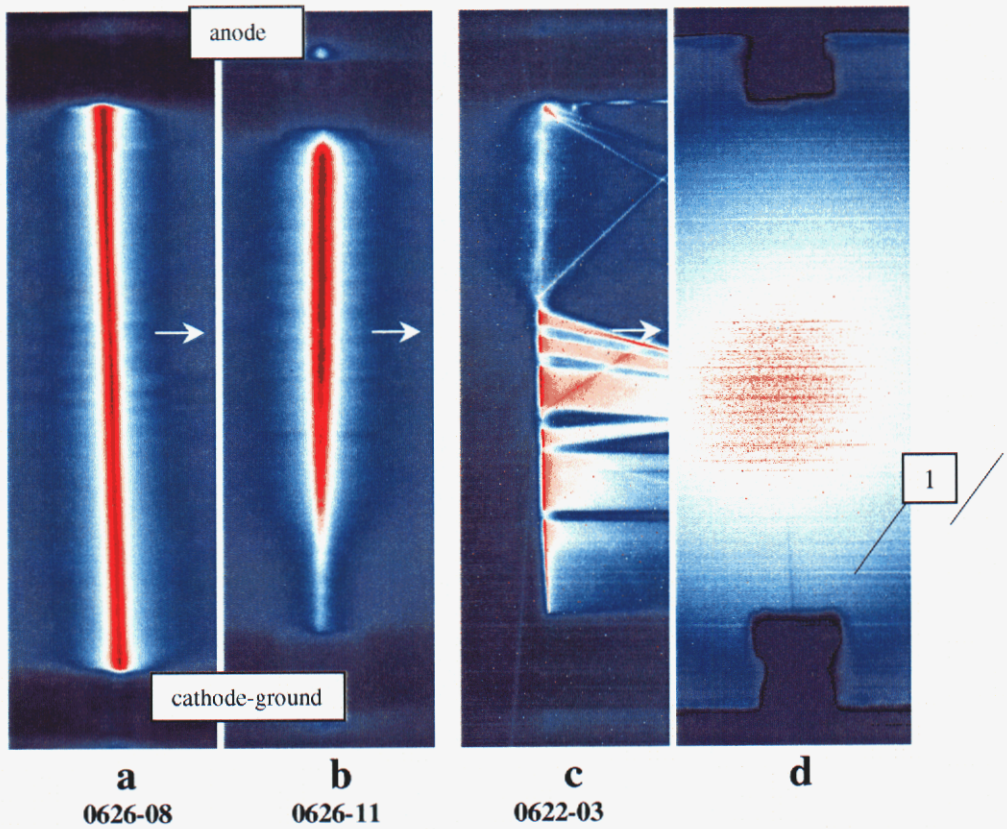

Figure 2. Time-integrated CCD images of 16.2-μm diameter and 2-cm long W wire explosions: (a) fast cylindrical explosion; (b) fast conical explosion; (c) slow explosion -- note off-axis arcing; (d) the cathode-anode gap after the shot (c) -- note portion of wire that has not been vaporized [1].The arrows on (a-c) show the cross-section imaged to the streak camera used to investigate the velocity of the wire expansion (Fig. 3).

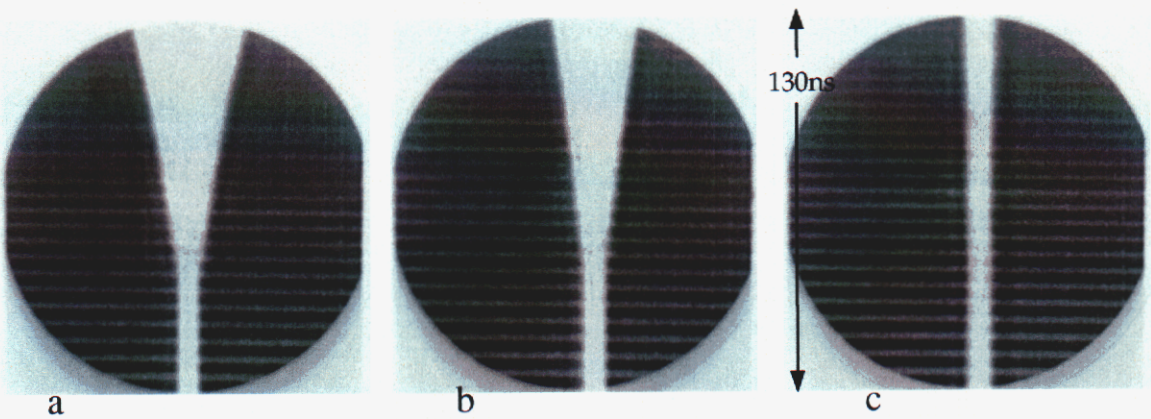

Figure 3. Radius-time (R-T) streaked laser-shadow images of the expansion in the middle of the 16.2-μm diameter W wire. R-T images (a), (b), (c) correspond to time-integrated images (a), (b), (c) in Fig. 2. Time flows from bottom to top.

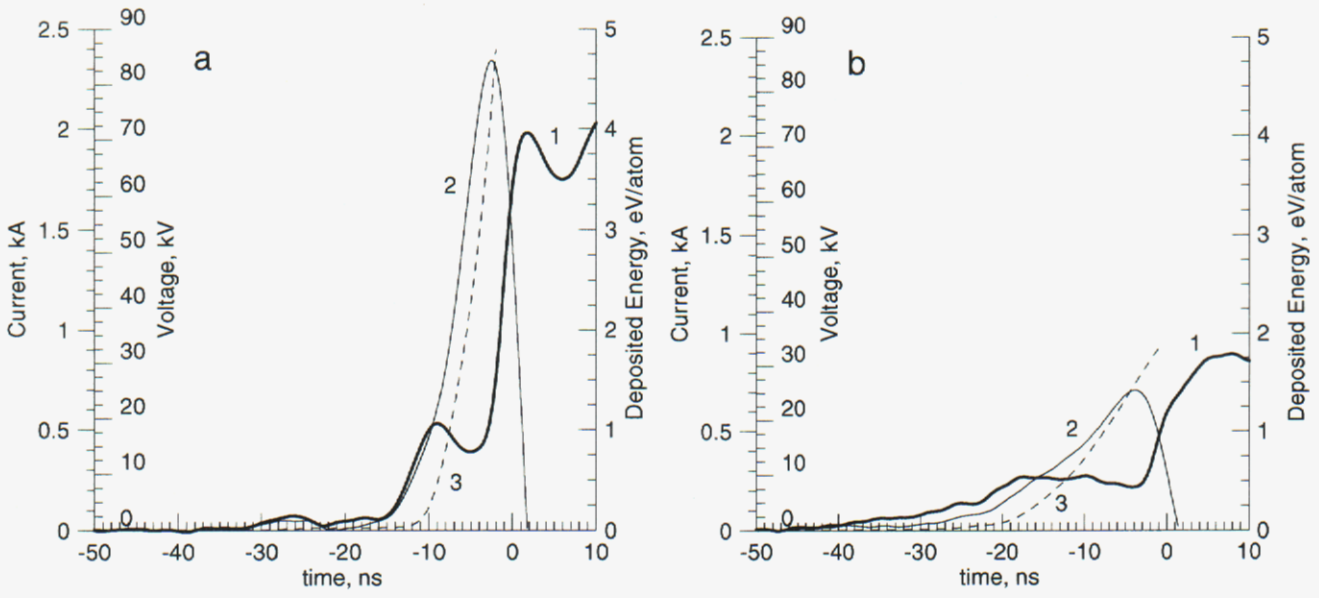

Figure 4. Current (1,heavy solid curve), voltage (2), and deposited joule energy (3, dashed curve) for: (a) a fast-pulse cylindrical explosion, and (b) a slow-pulse explosion.

Figure 5 displays the load resistivity and current density as a function of deposited energy for the fast cylindrical (1), conical (2), and slow (3) explosion modes. Initially, all three resistivity curves (1,2,3) essentially coincide. The only difference is the point at which flashover occurs - at 3 eV/atom, 2.5 eV/atom, and 1.5 eV/atom for the fast cylindrical (1), fast conical (2), and slow (3) explosion modes, respectively. For fast explosions the wire resistivity reaches 180-200 $\mu\Omega$·cm, far above the melting boundary [5], corresponding to the saturation plateau. In contrast, the resistivity with the slow-rising pulse only reaches 120 $\mu\Omega$·cm, below the melting boundary.

As seen in Figure 5, the current densities before and at flashover (1a,2a,3a) are substantial – around 2×10^8 A/cm^2 for fast-rising pulses, and 1×10^8 A/cm^2 for the slow-rising pulse. The magnetic field at the wire surface at flashover is 100 kG and 50 kG, for the fast- and slow-rising pulses, respectively. For a uniformly distributed current, this corresponds to a difference in magnetic pressure (B^2/μ_0), between the surface and the center of the wire of 80 MPa and 20 MPa, respectively – about 20% and 5% of the critical pressure for W. The higher magnetic field observed in the fast pulse mode may actually delay flashover, as evidenced by a higher deposited energy and higher current density.

The temporal evolution of the light emission from the fast cylindrical (1), fast conical (2) and slow (3) explosions is also shown in Figure 5. The extremely fast rising initial spike of light (at time t = 0) coincides in time with the rapid increase in current and the rapid decrease in voltage, i.e., with flashover. Fast explosions (especially in the cylindrical mode) yield the most light. Specifically, the radiation is over an order of magnitude stronger for wires driven by the fast-rising pulse. This is consistent with the

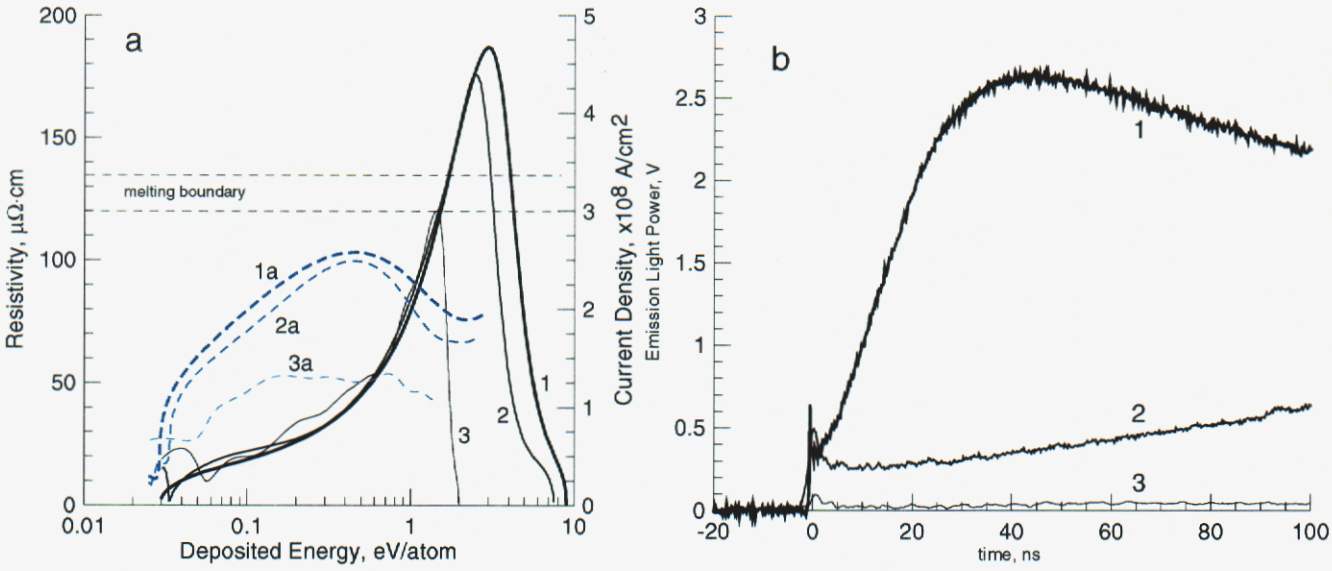

Figure 5. (a) Dependence on deposited energy of load resistivity (1,2,3) and corresponding current density (1a, 2a, 3a) for the fast cylindrical (1), fast conical (2), and slow (3) explosion modes of a 16.2-μm W wires. (b) Evolution of the emitted light power for the fast cylindrical (1), fast conical (2), and slow (3) explosion modes of these wires.

fact that a larger amount of energy is deposited into a wire driven by a fast-pulse Interestingly, the temporal shape of the radiation shown in Fig. 5(b) is typical only for W. Other substances give significantly different temporal shapes. For the fast cylindrical mode of explosion, the temporal shape of the radiation depends very strongly and distinctly on the wire material, but not much on the wire diameter.

The overall physical appearance observed between both the fast- and slow-current rise pulses does not appear to be very sensitive to wire diameter. This is shown in Figure 6 where tungsten wires ranging from 4μm to 25.6 μm in diameter were driven by both types of current pulse. For the fast-pulse explosion (170 A/ns), the Joule-energy deposition is uniform (i.e., cylindrical explosion) along the wire axis for all diameters, suggesting uniform current flow along the wire. On the other hand, in the slow-pulse explosion (22 A/ns), the energy deposition is not uniform; variegated off-axis arcing to the coaxial outer cylinder (transmission-line ground) occurs for all wire diameters and can take different forms (Figure 7). This indicates significant leakage of electrical energy, and lesser deposition of Joule energy inside the wire. For planar off-axis arcing, some of the initial wire is still observed after the shot, Figure 8, indicating that no vaporization occurred at that wire location. (The off-axis arcing is located preferentially in the direction of minimum distance between the wire and the coaxial outer cylinder - the wire load is slightly displaced from the axis of symmetry of the outer cylinder). The exception to the rule is the 4-μm-diameter tungsten wire, for which fast-pulse explosions result in a small amount of off-axis arcing about 90% of the time. In this case, the small radius of the wire promotes electron emission and arcing.

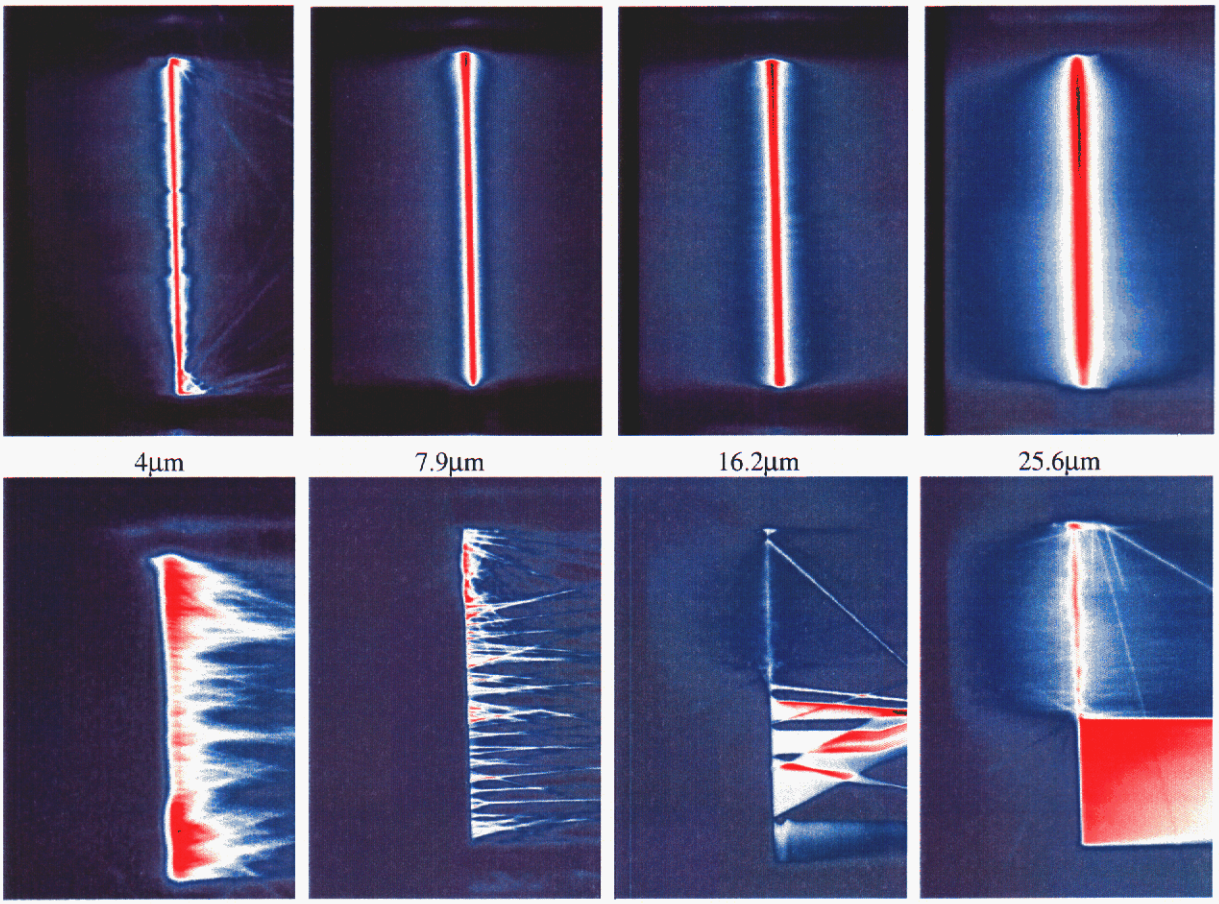

Figure 6. **(a)** Time-integrated CCD images of W wire explosions driven by a fast-rising pulse for four wire diameters, showing uniform energy deposition along the wire. The wire diameter is given below each image. **(b)** Images of slow-pulse explosions for the same wire substance and diameters. Off-axis arcing to opposite current cylinder indicates big leakage of electrical energy.

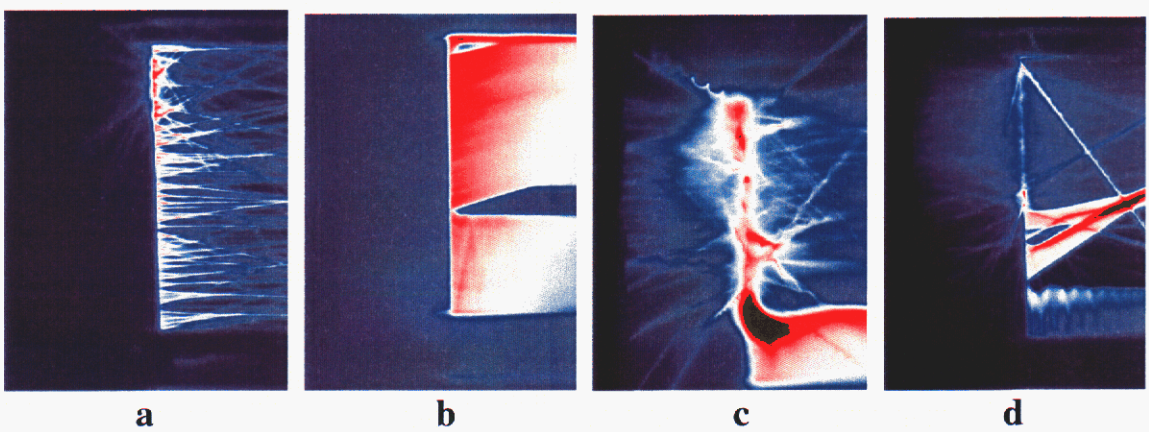

Figure 7. Different types of arcing for slow exploding W wire. Linear arc (a), planar arc (b), linear arc with kink instability (c), planar arc with aurora instability (d).

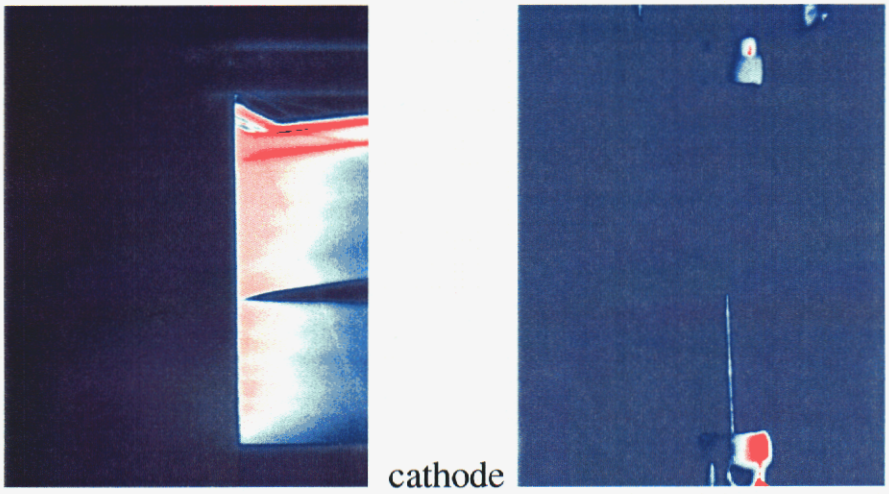

Figure 8. Slow-pulse explosion of 10.2-μm-diameter W wire: during explosion (a) and after explosion (b). After planar off-axis arcing cathode part of the wire has not been vaporized.

The expansion velocity of an exploding tungsten wire as a function of diameter is shown in Figure 9 for the fast-pulse case described above. This velocity was estimated using laser backlighting (532 nm and 905 nm) imaged to a streak camera (Figure10). As can be seen from the figure, the 10.2-μm diameter wire explodes with a velocity 0.33 km/s, while the thicker 20.3-μm wire explodes with a greater velocity of 1.12 km/s; the expansion velocity is inversely proportional to the wire diameter. Slow-pulse-driven tungsten wires explode with a velocity nearly 10 times less than the fast-pulse-driven ones.

The evolution of the deposited Joule energy per atom for fast-pulse explosions of tungsten wires as a function of wire diameter is shown in Figure 11. The specific Joule energy absorbed increases with decreasing wire diameter. Smaller-diameter wires thus absorb more Joule energy per atom yet still expand more slowly than larger-diameter wires. This suggest that the exploding wire material is acted upon by an ever increasing self-induced magnetic field, where the magnetic pressure is inversely proportional to the square of the wire diameter. For example, under the same current, a 4-μm-diameter wire will experience 25 times more magnetic field pressure than a 20-μm-diameter wire. During the fast pulse, 7.9-μm- and finer-diameter W wires experience a magnetic pressure in excess of the critical pressure of tungsten (337 Mpa). In this case, as the wire is heated, an overcritical phase transition from liquid takes place – liquid tungsten transforms into gas and plasma without separation into liquid and gas phases.

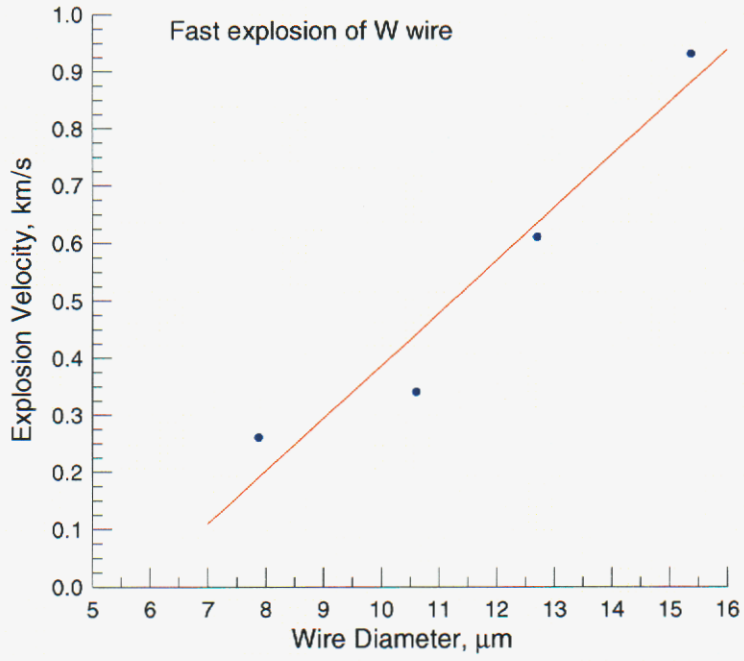

Figure 9. Dependence of the explosion velocity of fast exploding W wire from wire diameter.

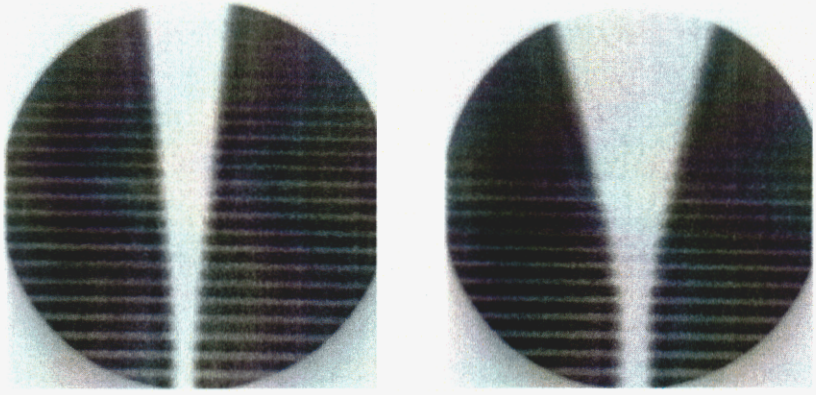

Figure 10. RT-diagram of fast exploded W wire with diameter (a) 10.2μm and (b) 20.3μm.

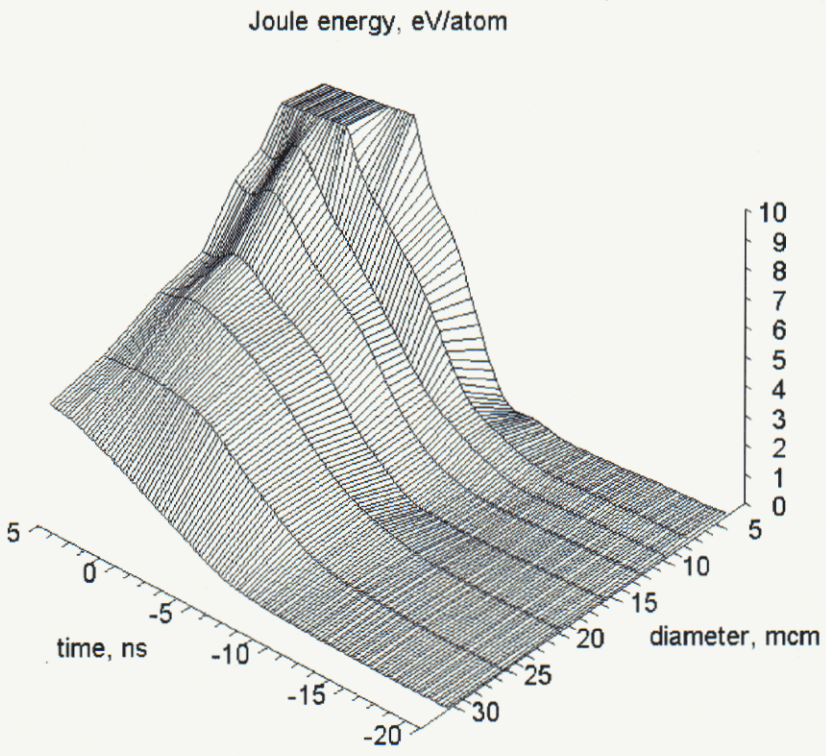

Figure 11. Evolution of the specific Joule energy for different diameters of fast exploding W wires

2.2.b Wire explosions: Effect of Heat of Vaporization

The wire initiation process was also studied using a variety of materials for the wire load. The experimental results show substantial differences in explosion properties based on the heat of vaporization of wire material. For materials with high heat of vaporization, such as Mo, Ti, Ni, and Fe, the trends are similar to that observed with tungsten wires and described in the previous section. For example, energy deposition is observed to vary dramatically between a fast- and slow-rising current drive. For the fast-rising current pulse, the energy deposition is uniform along the wire. Thicker wires comprised of the same material expand at a higher velocity but absorb less energy/atom than thinner wires. For the slower current rise, off-axis arcing is observed and the wire explosions are nonuniform.

For wires comprised of low-heat-of-vaporization materials, such as Au, Cu, Al and Ag, this off-axis arcing is never observed. Both rates of current rise give good quasi-cylindrical implosions and uniform deposition of energy along the wire. However, in slow-pulse explosions, the radial extent of the region of deposited energy is nearly twice as great as in fast-pulse explosions, although the light emitted is significantly less, and the velocities of wire expansion are slower (by a factor of 2-4, for Al and Au). Although no off-axis arcing was observed for these materials, arcing along the wire surface may cause some of the difference between fast and slow explosions.

The light emission (radiation) observed from a 20.3- μm diameter wire explosion using wires comprised of different substances is shown in Figure 12. With fast explosions (Fig.12a), the wire emission varies specifically with the material. For high-heat-of-vaporization materials, the optical emission increases with Z, while for low-heat-of – vaporization, the optical emission is much lower and substantially decreases over time. With slow explosions (Fig.12b), the wire evolution in terms of optical emission is much less sensitive to wire material.

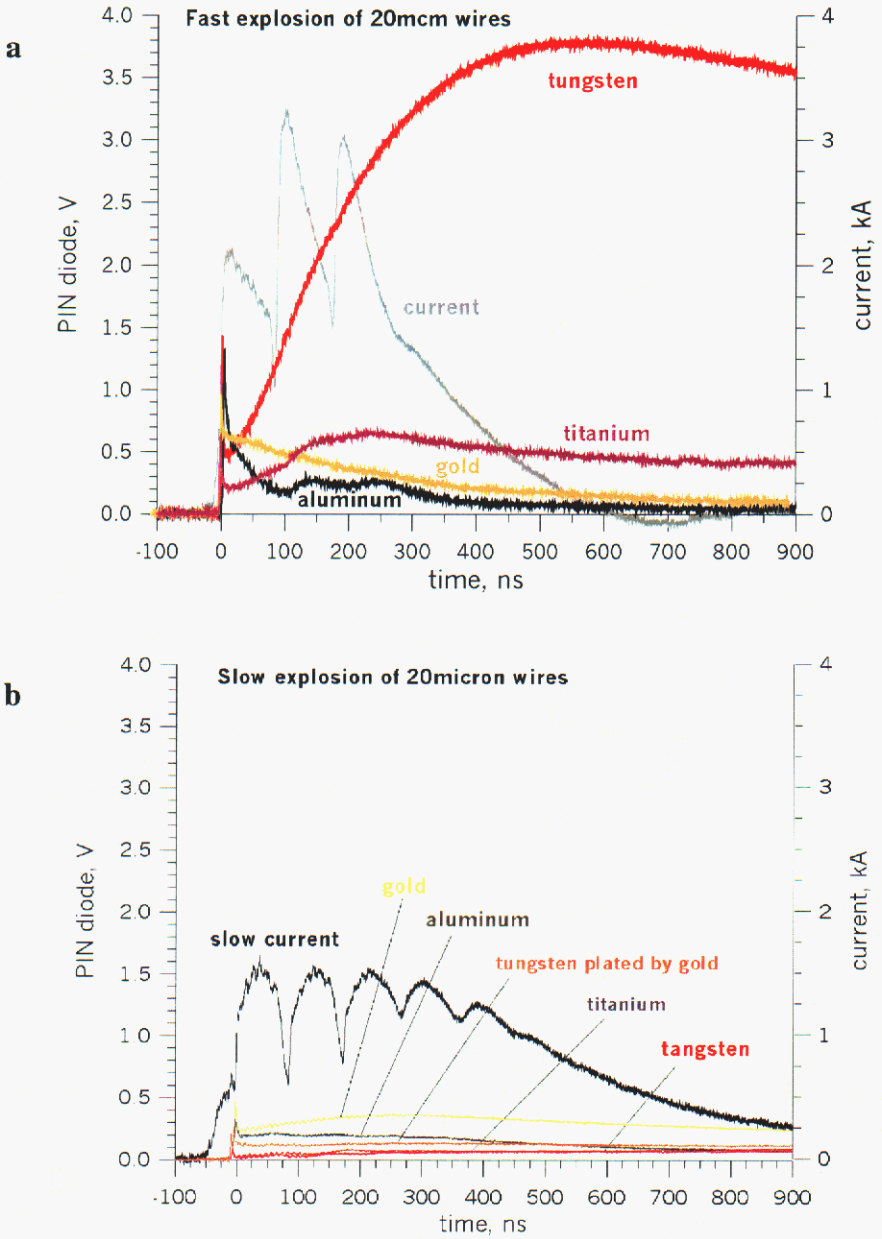

Figure 12. Emission of light for fast (a) and slow-pulse (b) explosion for 20.3-μm-diameter wires of different substances. Fast exploding wire gives bigger amplitude and characteristic light radiation.

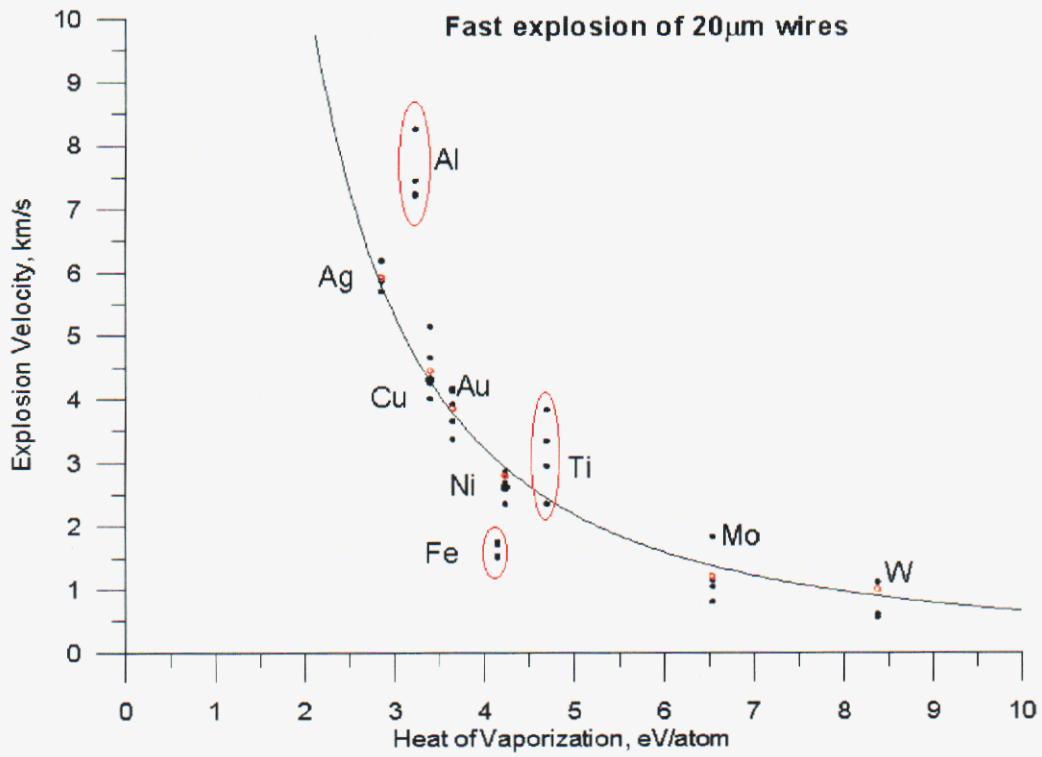

Figure 13. Dependence of the explosion velocity from heat of vaporization for fast exploding 20.3 μm wires of different substances. Al and Fe don't quite follow this relationship, possibly because of oxidation of the wire surface.

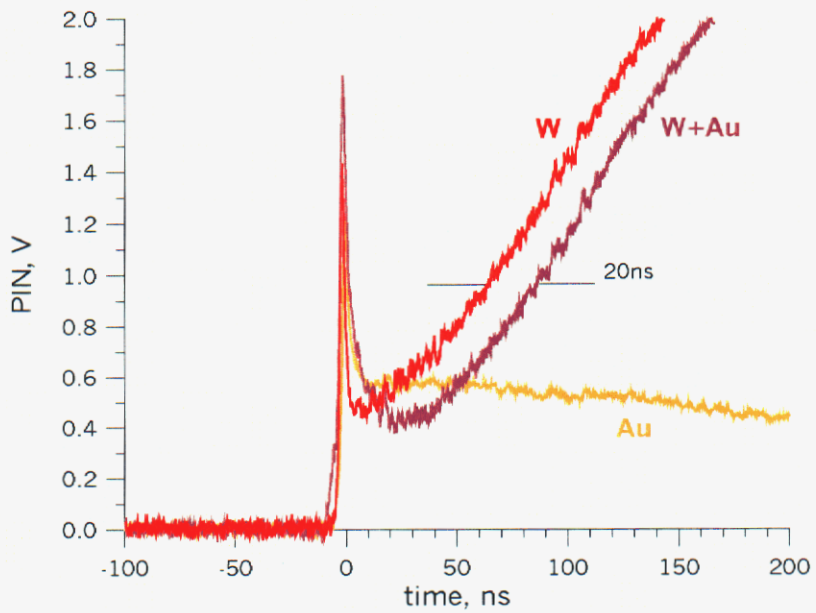

Figure 14. Emission of light from 20-μm-diameter W, Au-coated W wires for fast–pulse exploding mode. Gold coating burns out in 20 ns.

The velocity of expansion for the fast explosions of Figure 12a is shown in Figure 13. The data indicates that the velocity of wire expansion is inversely proportional to the square of the heat of vaporization of the wire material. Thus lower heat of vaporization materials, such as Al, expand much faster than W.

With Au-plated W wires, the two material types are combined and the explosion process exhibits behavior that is representative of each material. This is illustrated in Figure 14. Initially the light emission follows the behavior of an Au wire, and subsequently, with 20 ns retardation, the behavior of a W wire.

It is interesting to note that low-vaporization-energy-material wires quickly become completely transparent to 905 nm light for fast explosions (no opaque central region persists). Al wires become transparent sooner than Au or Cu wires. In contrast, an opaque central region persists at least 100 ns for slow-rising-current explosions. The expanding radial density distribution is thus markedly different for fast-rise and slow-rise current pulses, for the same wire and the same pulse energy.

An imaging optical spectrometer (Chromex 500is with a 100 grooves/mm grating, recorded by a CCD camera) was used to observe evidence of impurities in the explosion and to estimate the temperature. Time-Integrated, spatially-resolved (along the wire axis) spectra for fast explosions of 10.6-μm-diameter Al and 7.9-μm-diameter W wires are presented in Figures 15 and 16. Spectral lines from H and Cu impurities are observed, in addition to Al and W emissions. The ratio of the intensities of the Al^{+2} lines at 448 nm and at 452.9 nm suggests an electron temperature[2] of about 5 eV. The temperature of the Al appears higher near the anode and cathode than in between, in conjunction with the greater brightness near the anode and cathode as seen in the time-integrated CCD images of the Al wire explosions.

.

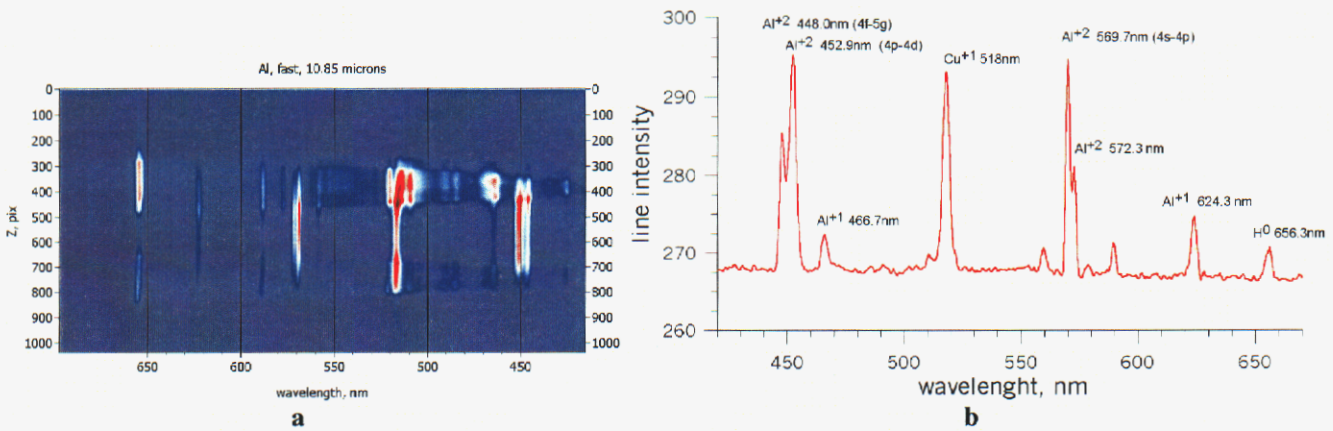

Figure 15. Spectra of fast exploding 10.9-μm-diameter Al wire (a), and spectral distribution of the line intensity in the middle cross-section (b).

[2] J. Bailey, Time-resolved optical spectroscopy measurements of pre-pulse plasma formation on Z, presented at the 26th IEEE ICOPS, Monterey, CA, June 20-24, 1999, USA.

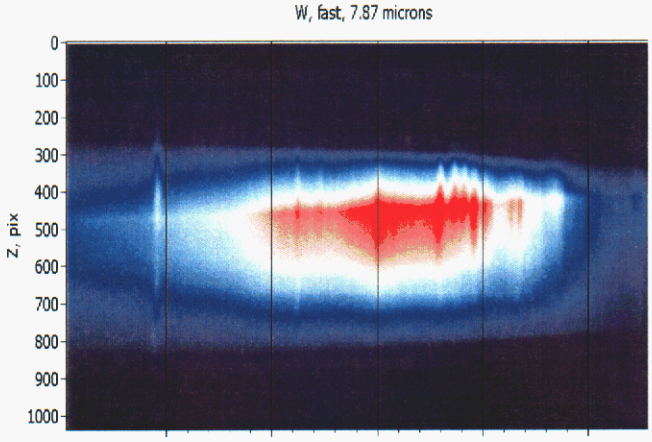

Figure 16. Spectra of fast-exploding 7.9-μm-diameter W wire.

3. Summary

The efficiency of heating wires driven by a high current is observed to improve dramatically with an increased rate of rise of the driving current. Wires were driven by a 12.6-J electrical pulse, with, alternately, a 40-80 A/ns current rise (4-8 kV/ns voltage rise) or a 10-20 A/ns current rise (0.8-1.6 kV/ns voltage rise). The slower rise is characteristic of the prepulse through individual wires on Z, where wires are exploded with a prepulse current that rises at 23-29 A/ns (7 kA/ns applied for 50 ns to an array of 240-300 fine wires).

The absorption of energy by high-current-driven wires is a two-stage process. Initially, the wire heats efficiently. Suddenly, a low resistance plasma forms around the wire, and most of the current is shunted into it. The voltage collapses, the power absorbed by the load decreases, and that power mostly goes into the plasma rather than into the wire. The heating of the wire becomes very inefficient and the load can contain a cold, even solid, core for a long time. Results presented in this report show that increasing the rate of rise of the driving current pulse (the fast current rise) can increase the efficiency of wire heating, i.e., energy absorbed. This is different from previous methods of increasing the energy deposition into a wire by delaying the onset of plasma formation, either by degassing the wire[3] or by insulating it[4]. This result dramatically increases the energy absorbed by all wires, whether untreated, degassed, or insulated. Remarkably, the time to flashover, from the start of the pulse, decreases only slightly for a substantially faster rising pulse. Thus the energy absorbed by the wire, prior to flashover, can be increased

[3] S.A. Pikuz, T.A. Shelkovenko, A.R. Mingaleev, D.A. Hammer, and H.P. Neves, Phys. Plasmas, 6, 4272 (1999).

[4] D.B. Sinars, T.A. Shelkovenko, S.A. Pikuz, M. Hu, V. M. Romanova, K.M. Chandler, J.B. Greenly, D.A. Hammer, and B.R. Kusse, Phys. Plasmas Lett. **7**, 429 (2000).

substantially by steepening the pulse rise. For example, heating a 16.2-μm-diameter tungsten wire with a fast pulse (~80 A/ns) produces a factor of 3 increase in energy deposition as compared to a slow pulse (~20 A/ns).

For fast explosions of W wires, the expansion velocity increases with the wire diameter. Smaller-diameter wires absorb more Joule energy per atom and still expand more slowly than larger-diameter wires. This indicates that their higher internal kinetic pressure is compensated by their higher inward magnetic field pressure, which is inversely proportional to square of the wire diameter. During the fast pulse, 7.9-μm- and finer-diameter W wires experience a magnetic pressure in excess of the critical pressure of tungsten (337Mpa). In this case, as the wire is heated, an overcritical phase transition from liquid takes place — liquid tungsten transforms into gas and plasma without separation into liquid and gas phases.

For substances with high vaporization energy (W, Mo, Ti, Ni, Fe, Au-plated W), a fast-rising current pulse deposits much more energy into a wire than does a slower-rising, Z-like pre-pulse. Furthermore, fast pulses result in a uniform deposition of energy along the wire and fairly quasi-cylindrical explosions. Slow pulses, on the other hand, tend to exhibit arcing. For both the fast-rising and slow-rising pulses, the load resistance increases many times from its room temperature value, as the wire heats, and then collapses in a few ns to a very small value when flashover occurs. As mentioned above, the time to flashover in both cases is comparable. Thus, with the slow-rising pulse through a 16.2-μm-diameter tungsten wire, the wire does not melt before flashover but disintegrates into solid parts, with a piece often remaining attached to the cathode after the discharge. In contrast, with the fast-rising pulse, a 16.2-μm-diameter tungsten wire melts before flashover, and subsequently explodes at ~1 km/s.

For wires comprised of materials with low vaporization energy (Au, Cu, Al, and Ag), the energy deposition along the wire is always observed to be uniform and the wires expand in a quasi-cylindrical nature regardless of the current rise. With the fast-rising current pulse, the expansion velocity of such wires is much higher than those with a high heat of vaporization, such as tungsten.

Overall, these series of experiments revealed characteristics of wire explosions that could be used to possibly modify wire array dynamics. For example, a fast-rising prepulse, in conjunction with preheated or insulated wires, could yield a plasma without a cold core and quicken the formation of a plasma shell from wire arrays. This could lead to an increased x-ray power from wire array implosions. The initial perturbations for the MRT instability in this case, most likely result from a nonuniform plasma distribution formed by the explosion of the wire array. Increased peak x-ray power at wire array stagnation correlates with decreased wire gap, presumably because this leads to earlier merging of the exploding wires and formation of a smoother plasma shell. Thus, efficient explosion of array wires by minimizing the cold-core / hot-corona phenomenon, would lead to earlier merging of the exploded wires into a plasma shell. This shell might be smoother, because perturbations would have less time to grow while the shell was forming. Future work will investigate such issues.

Distribution:

1	MS 0188	C.E. Meyers, LDRD Office (1030)
1	MS 1152	M.L. Kiefer (1642)
1	MS 1152	L.X Schneider (1643)
1	MS 1168	C. Deeney (1612)
1	MS 1178	D.D. Bloomquist (1630)
1	MS 1178	G.L. Donovan
1	MS 1178	F.W. Long (1637)
1	MS 1181	J. Asay (1610)
1	MS 1186	T. Mehlhorn (1674)
1	MS 1188	C. Olson (1600)
1	MS 1190	J.P. Quintenz (1600)
1	MS 1191	K. Matzen (1670)
1	MS 1193	J. Maenchen (1645)
1	MS 1193	J. Porter (1673)
5	MS 1194	M.R. Douglas (1644)
1	MS 1194	D. McDaniel (1640)
1	MS 1194	K. Struve (1644)
1	MS 1196	R.J. Leeper (1677)
1	MS 1391	D. Thompson (1614)
1	MS 9018	Central Technical Files (8945-1)
2	MS 0899	Technical Library (9616)
1	MS 0612	Review & Approval Desk (9612 for DOE/OSTI